Proposal for J-PARC 50 GeV Proton Synchrotron

3-Body Hadronic Reactions for New Aspects of Baryon Spectroscopy

K.H. Hicks (Ohio University), H. Sako (JAEA), spokespersons

Collaborators:

K. Imai, S. Hasegawa, S. Sato, K. Shirotori
(Japan Atomic Energy Agency, Tokai, Japan)

S. Chandavar, J. Goetz, W. Tang
(Ohio University, Athens, Ohio, USA)

J.K. Ahn, S.H. Hwang, S.H. Kim, S.J. Kim, S.Y. Kim, A. Hi, J.Y. Park and S.Y.Ryu
(Pusan National University, Pusan, Korea)

H. Fujioka, S. Nakamura and M. Niiyama
(Kyoto University, Kyoto, Japan)

K. Ozawa
(KEK, Tsukuba, Japan)

K. Joo, N. Markov, N. Harrison, T. O'Connell, E. Seder
(University of Connecticut, Storrs, Connecticut, USA)

W.J. Briscoe, F. Klein, I. Strakovsky, R. Workman
(George Washington University, Washington, DC, USA)

R. Schumacher
(Carnegie Melon University, Pittsburgh, PA, USA)

D.M. Manley
(Kent State University, Kent, Ohio, USA)

L. Guo
(Florida International University, Miami, Florida, USA)

P. Cole
(Idaho State University, Pocatello, ID, USA)

T.S.-H. Lee
(Argonne National Lab, Chicago, Illinois, USA)

T. Sato and H. Kamano
(Osaka University, Osaka, Japan)

Y. Azimov
(Petersburg Nuclear Physics Institute, St. Petersburg, Russia)

V. Shklyar
(University of Giessen, 35392 Giessen, Germany)

Abstract

The nucleon resonance spectrum holds fundamental information about non-perturbative QCD. However, the resonance spectrum is not easily extracted from experimental data due to the large widths of the overlapping resonances. Precise data on both photoproduction and hadronic reactions are needed in order to separate the nucleon resonances using a partial-wave analysis (PWA). Recent theoretical advances have shown the importance of coupled-channels effects in a PWA, and that it is necessary to complement the high-quality data on the $\pi N \to \pi N$ channel with similar-quality data for the $\pi N \to \pi\pi N$ and $\pi N \to KY$ reactions. The latter reactions were measured with only modest precision about three decades ago. With J-PARC, it is now possible to make precise measurements of these reactions, and hence extract the nucleon resonance spectrum. One exciting development comes from recent lattice QCD calculations, which predict that hybrid baryons (with gluonic excitations in the three-quark system) should exist. If hybrid resonances exist, it is essential to get hadronic data on $\pi N \to \pi\pi N$ to use in dynamical coupled-channels PWA that provide the best chance of reliable resonance extraction from the data. Preliminary indications from photoproduction data at CLAS suggest that an extra resonance, in addition to the known quark-model resonances), has been seen in reaction $\gamma p \to \pi^+\pi^- p$ at a mass close to that predicted from the lattice for a hybrid baryon. Whether this is a regular baryon resonance or a hybrid baryon resonance, precise hadronic data are needed to untangle it from other nearby (overlapping) baryon resonances having large widths. We propose to measure the $\pi N \to \pi\pi N$ and $\pi N \to KY$ reactions at J-PARC with sufficient precision to search for baryon resonances. The proposed experiment will use the K1.8 beamline to span a range in the center-of-mass energy W (from 1.54 to 2.15 GeV) with a large-acceptance Time Projection Chamber (TPC) spectrometer. This TPC is being designed by the JAEA hadronic physics group for use in another J-PARC experiment to search for the H-dibaryon (P42). With only minor modifications for the target, the same hardware can be used for the experiment proposed here. **We request a total of 45 shifts on the K1.8 beamline to measure the reactions $\pi N \to \pi\pi N$ and $\pi N \to KY$.**

1 Introduction

One of the primary reasons for studying the nucleon resonance spectrum is to get a deeper understanding of QCD. Just like the case of the excited spectrum of hydrogen (Lyman series, Balmer series, etc.) led to a deeper understanding of the electromagnetic interactions in the atom, now a precise determination of the excited spectrum of the nucleon will lead to a deeper understanding of QCD. In particular, we need to know the pole positions and widths of nucleon resonances to test calculations of non-perturbative QCD. This information requires a theoretical framework to do a partial-wave analysis on precise data from hadron and photon beams.

Over the past decades, there has been intense effort to understand the nucleon resonance spectrum. Much of the early work was done using just hadronic beam data, often from pion beams and hydrogen bubble-chamber detectors from the 1970s. This led to the so-called "missing resonance" problem [1], because many of the nucleon resonances predicted by the quark model [2] were not found by partial-wave analyses of these hadronic-beam data. Although the quark model was extremely successful in some ways, such as calculations of the baryon magnetic moments and masses of the ground-state baryons, the quark model could be seen as a disappointment in calculations of the nucleon resonance spectrum. One of the primary motivations for building the CLAS detector at Jefferson Lab, with the collection of precise photoproduction data, was to resolve the problem of the excited states of the nucleon. After more than ten years of effort, the problem remains unsolved.

In recent years, the realm of calculation has shifted from the simple quark model to computationally complex calculations on the lattice. Lattice calculations for the spectrum of hadrons, both meson and baryons, has progressed to the point where they can predict both the masses of known resonances and also predict new nucleon resonances at higher mass. While one could easily discount the quark model calculations for its simplistic approach (with many approximations), the lattice calculations are direct predictions from QCD. We now have the ability to test QCD directly when the pole positions of the nucleon resonances if precise experimental data are available. Currently, very good data on $\pi N \to \pi N$ are available, but as we show below, precise data for the $\pi N \to \pi\pi N$ reaction are lacking.

The outline of this proposal is as follows. First we describe new lattice calculations that predict nucleon resonances that are primarily of hybrid-baryon character. Next, we show that the data from photoproduction reactions alone are not sufficient to deduce the nucleon resonance spectrum, due to the presence of final-state interactions. A theoretical model, using a dynamical coupled-channels calculation, is next described, which has been used to find the resonance poles from data on both hadronic and photoproduction reactions. High-precision data from JLab shows that large discrepancies exist

between data and calculations using resonances in the Particle Data Group (PDG) listings, showing the need for new nucleon resonances. Hence, data from J-PARC are central to solving the long-standing problem of the nucleon resonance spectrum, since these data are essential to constrain properly the coupled-channels analysis. Finally, an experimental plan at the Hadron Experimental Facility of J-PARC is presented for the K1.8 beamline using a large-acceptance, high-rate TPC detector being built by the JAEA hadron physics group.

The international collaboration between Jefferson Lab and J-PARC, with each facility taking precision data that will be used in the search for new nucleon resonances, is a key step toward the goal of finding new aspects of baryon spectroscopy.

2 Physics Motivation

It is well known that QCD is a strongly interacting theory of quarks and gluons. Yet most of the attention has been centered on the quarks (and not the gluons) in calculations of the spectrum of mesons and baryons. Many popular quark models are presented in standard textbooks, where the quarks are confined by potentials representing approximations to the gluon field. However, since the gluons are strongly coupled to the quarks, it is possible to have gluonic excitations in the spectrum of resonances. In fact, recent calculations using lattice QCD have shown that such hybrid baryons are expected as part of the spectrum of nucleon resonances [3]. In order to test these theoretical predictions, data from both hadronic reactions at J-PARC and photoproduction reactions at Jefferson Lab (JLab) will be necessary to unfold the nucleon resonance spectrum from the experimental data.

The lattice calculations of interest here were done at JLab by the Hadron Spectrum Collaboration [3]. Using a large basis of interpolating fields, they were able to separate the lattice mass eigenstates into spin-parity assignments along with the relative sizes of their matrix elements corresponding to a non-relativistic subset of operators. The results are shown in Fig. 1, where the vertical axis is the mass calculated for a pion mass of 396 MeV. The true masses will become smaller as the light quark mass is reduced. At present, these calculations give a reasonable spectrum with the nucleon mass at about 1.2 GeV and the first band of conventional (qqq) nucleon resonances near 2.3 GeV, shown by the grey boxes. The new aspect of this resonance spectrum is several resonances near 2.6 GeV, shown by the blue boxes, where the lattice projection operators show as having gluonic excitations (details are given in Ref. [3]). This is the first time that "hybrid" baryons have been predicted from the lattice. While more definitive calculations are in progress using more realistic pion masses, the masses of the hybrid baryons relative to the

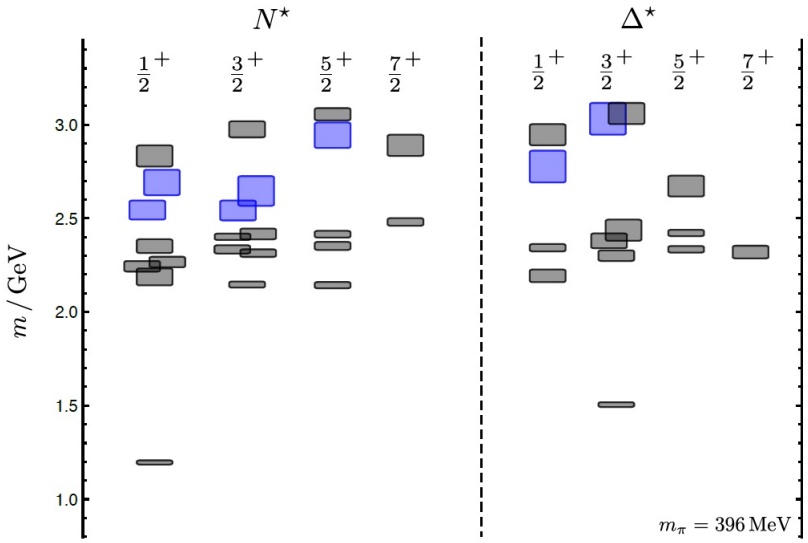

Figure 1: Nucleon resonances calculated on the lattice, where conventional qqq states are shown by the grey boxes and hybrid baryons are shown by the blue boxes (from Ref. [3]).

conventional baryons are not likely to change much. Now that these hybrid baryons have been predicted, the question is how they decay and whether experiments can confirm these predictions from the lattice QCD spectrum.

2.1 Dynamical Coupled-Channels Model

Equally important are theoretical advances in the dynamical coupled-channels calculations [4]. In this model, the physical nucleon resonances are mixtures of a qqq core plus a meson cloud and a virtual five-quark meson-baryon molecule. The meson-baryon component is essential to complete the Fock tower of states in the wave-functions of the nucleon resonances. A practical aspect of the meson-baryon component is that rescattering (final-state interactions) can occur, and so the resonance pole positions cannot be determined accurately without doing the full dynamical calculation.

As an example, consider the reaction $\pi N \to \pi\pi N$. The equations of the scattering T-matrix are shown schematically in Fig. 2 in the model of Ref. [5]. Notice the second term, $v_{MB,\pi\pi N}$, which shows the rescattering of an intermediate meson-baryon state leading to the $\pi\pi N$ final state. These final-state interactions are not small effects, as shown in Fig. 3. In that figure we see that without the coupled-channels terms, the calculations deviate substantially from the total cross sections. The effects are equally dramatic in the invariant mass distributions (see Ref. [5]). However, no differential

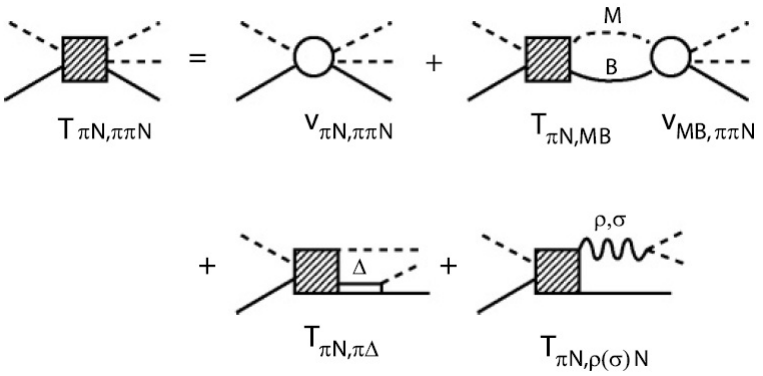

Figure 2: Graphical representations of the scattering amplitudes used in the dynamical coupled-channels calculation of Ref. [5].

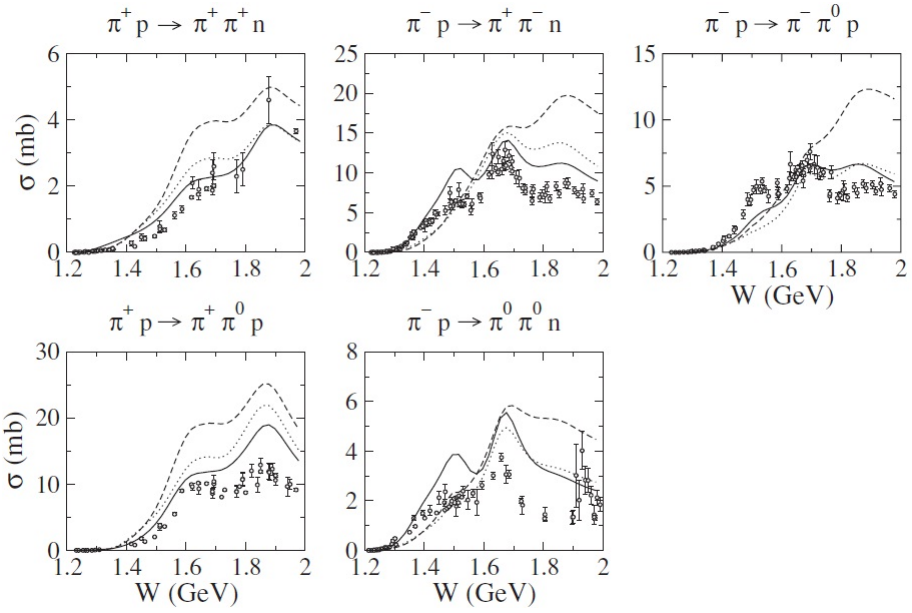

Figure 3: Coupled channels effects compared with data on the reaction $\pi N \to \pi\pi N$. Solid curves are the full calculations and the dashed curves have no coupled-channels terms, from the calculation of Ref. [5]. The dotted curve is explained in that reference.

	$M^0_{N^*}$	M_R	Location	PDG
S_{11}	1800	(1540, 191)	$(uuuupp)$	(1490–1530, 45–125)
	1880	(1642, 41)	$(uuuupp)$	(1640–1670, 75–90)
P_{11}	1763	(1357, 76)	$(upuupp)$	(1350–1380, 80–110)
	1763	(1364, 105)	$(upuppp)$	
	1763	(1820, 248)	$(uuuuup)$	(1670–1770, 40–190)
P_{13}	1711	···		(1660–1690, 57–138)
D_{13}	1899	(1521, 58)	$(uuuupp)$	(1505–1515, 52–60)
D_{15}	1898	(1654, 77)	$(uuuupp)$	(1655–1665, 62–75)
F_{15}	2187	(1674, 53)	$(uuuupp)$	(1665–1680, 55–68)
S_{31}	1850	(1563, 95)	$(u\text{-}uup\text{-})$	(1590–1610, 57–60)
P_{31}	1900	···		(1830–1880, 100–250)
P_{33}	1391	(1211, 50)	$(u\text{-}ppp\text{-})$	(1209–1211, 49–51)
	1600	···		(1500–1700, 200–400)
D_{33}	1976	(1604, 106)	$(u\text{-}uup\text{-})$	(1620–1680, 80–120)
F_{35}	2162	(1738, 110)	$(u\text{-}uuu\text{-})$	(1825–1835, 132–150)
	2162	(1928, 165)	$(u\text{-}uuu\text{-})$	
F_{37}	2138	(1858, 100)	$(u\text{-}uuu\text{-})$	(1870–1890, 110–130)

Figure 4: Table of resonance masses, M_R, listed as $(Re, -Im)$ pole positions, compared with the PDG values, from the calculation of Ref. [7]. The third column, Location, is not important for the comparison (see [7] for details).

cross sections for the angular distributions are available from these $\pi\pi N$ data for comparison with calculations. As will be shown below, ambiguities in fits to the resonance pole positions can be resolved if high-precision data for the $\pi N \to \pi\pi N$ reaction were available.

The important point to take away from the above discussion is that the nucleon resonance poles require sophisticated dynamic coupled-channels calculations, with parameters that need high-quality data from a variety of hadronic reactions. In particular, data from $\pi N \to \pi\pi N$ are not sufficient. Most of the three- and four-star nucleon resonances in the Particle Data Group (PDG) listings [6] were determined primarily from partial-wave analysis of just the $\pi N \to \pi N$ data. However, many of these resonances have strong decay branching ratios to the $\pi\pi N$ final state [6]. To do a more complete analysis requires fitting all of the reaction data (for both hadronic beams and photon beams) simultaneously using coupled-channels effects, which has been done recently by the EBAC theory group at Jefferson Lab [7]. The results of that calculation are captured in Fig. 4, showing general

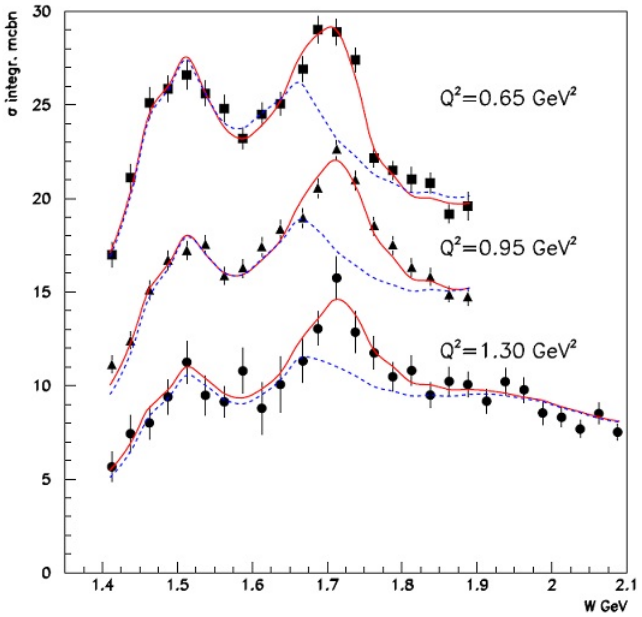

Figure 5: Data from the CLAS Collaboration for the reaction $ep \to e'\pi^+\pi^- n$ at W=1.7 GeV from Ref. [8].

agreement with the PDG values, but with some differences. The differences are important, because a precise comparison of lattice calculations and the pole positions of the nucleon resonance spectrum can only be achieved when coupled-channels effects are taken into account.

To further demonstrate the above points, data from the CLAS detector for two-pion photoproduction [8] are shown in Fig. 5. Here, two curves are shown, where the dotted line is a calculation that includes only the known PDG nucleon resonances, whereas the solid curve has a new P_{13} resonance that couples strongly to 2π decay. This state is not seen in the list of Fig. 4 because the two-pion photoproduction data were not included in that fit. As noted in the EBAC paper [7], a more comprehensive fit that includes all reaction data with $\pi\pi N$ final states will be required to complete the list of resonances. However, the lack of hadronic data for $\pi N \to \pi\pi N$ for beam energies above 0.75 GeV/c makes this task very difficult, with ambiguous solutions for the resonance pole positions [9]. To illustrate the importance of the 2π decay, the widths for the EBAC resonance decays (still preliminary) are shown in Fig. 6. For many resonances, over half of the decay branching fraction goes into the 2π channel.

It is difficult to believe that the nucleon resonance problem (or the question of hybrid baryons) will be solved unless there are more reliable data for the hadronic reaction $\pi N \to \pi\pi N$. The importance of these data has been

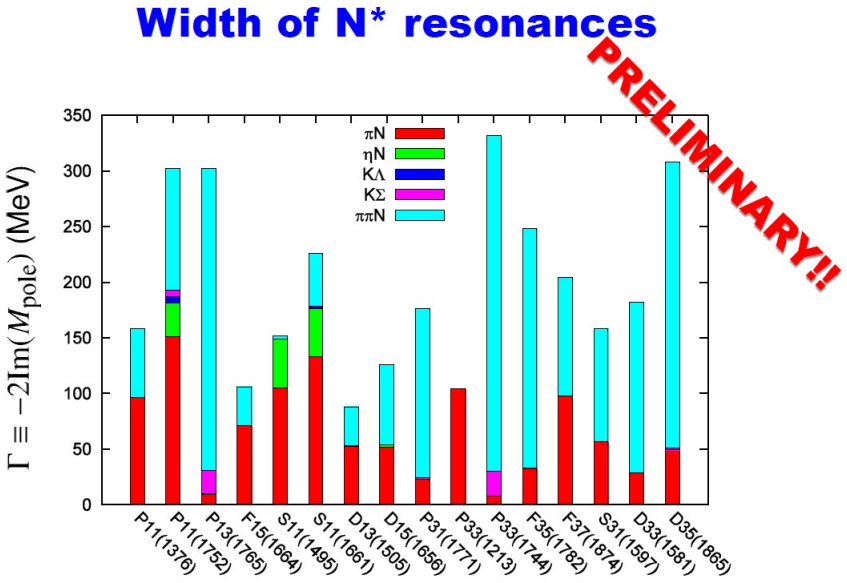

Figure 6: Preliminary results from the EBAC fits, showing the decay widths into various final states, from Ref. [5].

overlooked for nearly three decades, and now J-PARC is the only facility in the world that can address this deficiency. If we want to know the nucleon excitation spectrum, which has a fundamental link with QCD, then this cannot be done properly without measuring the above reaction. The exciting possibility that hybrid baryons could exist, and hence that gluonic excitations are a universal aspect of strongly interacting particles, may end in a fruitless search without the proposed data to constrain the coupled-channels analyses.

2.2 Isospin Amplitudes

From isospin invariance, the amplitudes for the different charge states of the $\pi N \to \pi\pi N$ reaction can be written in terms of four independent isospin amplitudes. Using the standard notation $A_{2I,I'}$ where I is the isospin of the initial-state πN system and I' is the isospin of the two final-state pions, the amplitudes of the measurable reactions are [10]:

$$A(\pi^- p \to \pi^0\pi^0 n) = \frac{2}{3\sqrt{5}}A_{32} + \frac{\sqrt{2}}{3}A_{10} \quad (1)$$

$$A(\pi^- p \to \pi^+\pi^- n) = \frac{1}{3\sqrt{5}}A_{32} - \frac{\sqrt{2}}{3}A_{10} + \frac{1}{3}A_{31} - \frac{1}{3}A_{11} \quad (2)$$

$$A(\pi^- p \to \pi^0\pi^- p) = -\frac{1}{\sqrt{10}}A_{32} + \frac{1}{3\sqrt{2}}A_{31} + \frac{\sqrt{2}}{3}A_{11} \quad (3)$$

$$A(\pi^+ p \to \pi^0 \pi^+ p) = -\frac{1}{\sqrt{10}} A_{32} - \frac{1}{\sqrt{2}} A_{31} \quad (4)$$

$$A(\pi^+ p \to \pi^+ \pi^+ n) = \frac{2}{\sqrt{5}} A_{32} \ . \quad (5)$$

Only the latter four reactions, which have two charged tracks each, can be measured using the large-acceptance TPC setup at J-PARC.

The four isospin amplitudes in the above equations are complex. Neglecting an overall phase and realizing that only relative phases are important, there are six independent constants for each center-of-mass energy W. Since there are only five reaction channels, one needs additional information from, for example, polarized target data. However, reasonable assumptions can be made using chiral symmetry near threshold [10]. Assuming a smooth energy-dependence for the amplitudes (and their relative phases), one can solve for the amplitudes using a partial-wave analysis. Details are given in Ref. [12]. To do this, it is important to have data in a range of small steps in W, which is what we propose to do at J-PARC.

2.3 Previous $(\pi, 2\pi)$ Data

Most of the data for the $\pi N \to \pi\pi N$ and $\pi p \to KY$ reactions were taken over 3 decades ago. At that time, the experimental techniques were far behind today's standards. At J-PARC, the beam intensities are almost 1000 time higher than in the 1970s, and detector technologies (along with data acquisition systems) have similarly advanced. Perhaps more important is that modern technology has vastly reduced human error in data analysis, unlike the methods employed when data for the above reactions were taken. Considering the importance of these data to understand the spectrum of nucleon and hyperon resonances, it is perhaps surprising that no modern experiment has undertaken to improve the precision and coverage of these reactions in the nucleon resonance region.

For the $\pi^- p \to \pi\pi N$ reaction, one of the more recent publications is given in Ref. [11]. (Earlier references are cited in this publication.) These data were taken with the Saturn accelerator in Saclay during the early 1970s. Ref. [11] has six beam energies between 1.505 and 1.739 GeV. An earlier measurement by the same group (cited in Ref. [11]) has four energies between 1.39 and 1.53 GeV. All of these data were collected using a bubble chamber, for a total of about 330,000 pictures (which were individually scanned and the resulting tracks entered into a computer). Their publication states: "A rather large electron and muon beam contamination made an absolute determination of cross sections impossible" [11]. Hence, only relative quantities, such as angular distributions, are possible to extract from these data, so the goal of obtaining coupling constants for the hadronic vertices becomes quite difficult.

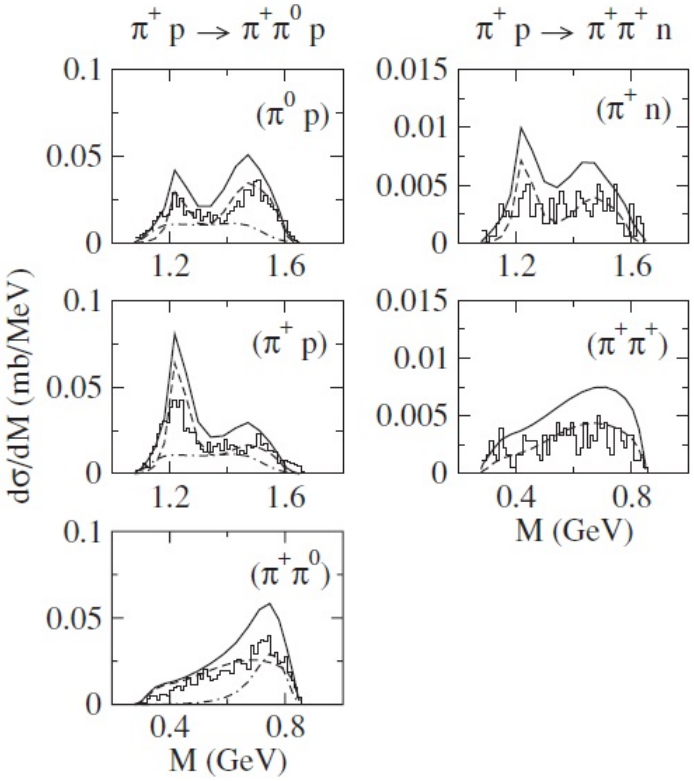

Figure 7: Mass projections of the data from Ref. [11], with curves showing the predictions of the calculation by Ref. [5] (solid) and contributions from $\pi\Delta$ (dashed) and ρN (dot-dashed) decay channels. The data have been normalized to the average total cross section from other measurements, and so the overall vertical scale has some uncertainty.

In Ref. [5], theoretical calculations from the dynamical coupled-channels model are compared with the shapes of the mass distributions from the above data [11]. For this exercise, the data have been normalized (using total cross sections from other measurements having nearly the same center-of-mass energy, W). As shown in Ref. [5], the agreement of the one-dimensional mass shape is fairly good, see Fig. 7. Of course, the normalization of the solid curve, which is not fit to these data (it comes from the model parameters fit to πN elastic data), is not reliable due to the *ad hoc* procedure used to normalize the data.

The data have poor statistics, and so only very sparse two-dimensional plots are possible [9]. So it is not possible to know if there are correlations in the data between various hadronic resonances, such as the ρ (in the invariant mass of two pions) and the Δ (in the invariant mass of a proton and pion). Such correlations are important to understand, as some features of these mass spectra may come from kinematical reflections of resonances in other mass combinations.

For the proposed data, multi-dimensional binning of the data is possible, so that correlations between, say, the two-pion mass, $M(\pi\pi)$ versus the center of mass angle $\theta_{c.m.}$ would be possible to explore, such as correlations between ρ-meson production and its decay angle in the Godfrey-Jackson rest-frame. In addition, Dalitz plots, such as $M(\pi\pi)$ vs. $M(\pi N)$, could be studied to separate meson resonances from nucleon resonances. Clearly, no multi-dimensional binning was done in Ref. [11].

There have been some recent data for the $\pi N \to \pi\pi N$ reaction, but almost all of these data are at lower-energy (below beam momenta of 0.75 GeV/c). Those data are tabulated in the references of Ref. [5]. The goal of the near-threshold measurements is to study the π-π phase shift through final-state interactions, and comparisons to Chiral Perturbation Theory (CPT). While this is an important goal, it has little to do with the proposed measurements here, where the focus is on the study of nucleon resonances.

In addition to Ref. [11], there are several measurements of the $\pi N \to \pi\pi N$ reaction prior to 1974. These references are tabulated in Ref. [12] and also in Ref. [13]. Many references in the latter are at beam momenta above 2.0 GeV/c, which is higher than we can currently measure using the K1.8 beamline at J-PARC, and so those measurements do not compete with the present proposal. In any case, all of the data prior to 1974 are of poor statistical precision and do not uniformly cover the range of beam momenta between 0.75 and 2.0 GeV/c, corresponding to the W range of the nucleon resonances [12].

2.4 Previous (π, K) Data

Some resonances are expected to couple strongly to strange-particle final states. In the classic paper by Capstick and Roberts [1], which discusses the "missing resonance" problem, their theoretical calculations predict that a few resonances would decay strongly to the $K\Lambda$ final state, with only a very small branching ratio to the πN final state. Those resonances could have been missed in partial-wave analysis of single-pion scattering. To do a proper search for nucleon resonances, one also needs good data for the reaction $\pi N \to KY$, where Y is either a Λ or a Σ hyperon.

As mentioned previously, there are strong coupled-channels effects in photoproduction [4], and hence data on the hadronic reaction $\pi N \to KY$ is necessary to carry out a combined search for nucleon resonances using both hadronic and photoproduction data. This is the goal of the EBAC effort [7] at Jefferson Lab. For the EBAC effort to succeed, all significant coupled channels need to be measured. This includes the $\pi N \to KY$ channel.

Most of the world's previous data on the $\pi N \to K\Lambda$ reaction were taken at the 7 GeV proton accelerator NIMROD, using optical spark-chambers and other experimental equipment common in the late 1970s. These data are of modest statistical precision, and span the center-of-mass range from $1.7 < W < 2.3$ GeV [14]. The cross sections are not small, with values of a few-hundred microbarns. This reaction could be measured at J-PARC, with considerably better accuracy, simultaneously with the two-pion final state. Experimental details on the trigger and count rates will be given in the next section.

As an example of the importance to measure the KY final state, a partial-wave analysis of the NIMROD data shows evidence for a new resonance in the P_{11} wave at a mass between about 1.67 GeV and 1.73 GeV that was not seen in the single-pion analysis [14]. In photoproduction data from the CLAS detector at Jefferson Lab, total cross sections to the $K\Lambda$ final state also clearly show a peak near $W = 1.7$ GeV, which they attribute to a P_{11} resonance [15]. Additional evidence for another P_{11} resonance near a mass of 1.9 GeV, which was not seen in the partial-wave analysis of the hadronic data [14], is also seen in the CLAS data. However, recent PWA solutions which include polarization data favor a P_{13} wave resonance at 1.9 GeV [24]. The photoproduction data is now much more precise than the existing hadronic data, even though the hadronic cross section is about a factor of 100 larger. In any case, both data sets are necessary to isolate new nucleon resonances in a proper coupled-channels analysis.

As for the case of $(\pi, 2\pi)$ data, there have been recent measurements of the (π, K) at higher W [17, 18], but no new data in the resonance region. Here, we proposed to take new high-statistics data for the $\pi N \to KY$ reaction. These data come "for free" in the same data set as for the $\pi N \to \pi\pi N$ data.

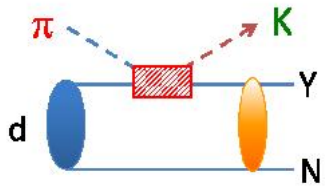

Figure 8: The $\pi d \to KYN$ reactions.

The KY final state is a two-body reaction, so two-dimensional projections are not necessary. Hence lower count-rates are not a problem.

2.5 Theoretical connection with YN scattering

Recent developments of the Lattice QCD techniques and the computational resources have opened a new era of the physics of hadrons and nuclei: direct evaluation of the baryon-baryon interactions from QCD has been achieved in the SU(3) limit and heavier pion masses [19]. Evaluation of lattice data at physical pion masses is becoming a reality with the K-computer at Kobe and other massive computer systems around the world, such as the one at Jefferson Lab. Precise extraction of the baryon-baryon interactions (in particular, the YN and YY interactions) from the analysis of the experimental data is also urgent, so as to make a comparison with the Lattice QCD results.

Measurements of the $\pi N \to KY$ reactions can be a key to understanding YN interactions. Recently, a new project [21] on determining the YN interactions through an analysis of $\pi d \to KYN$ reaction (Fig. 8), has been started. There, the dynamical couple-channels approach developed in Ref. [20] is applied to describing the elementary hyperon production processes (red shaded box in Fig. 8). Combined with the well-established deuteron wave function, the YN interactions are determined by analyzing the available data of the $\pi d \to KYN$ reactions. The reliability of the extracted YN interactions depends on the model describing elementary hyperon-production processes. To make the model reliable, high precision data on the $\pi N \to KY$ reactions are required because the model parameters cannot be fixed without those reaction data.

Kinematical coverage of available $d\sigma/d\Omega$ (P) of the $\pi^- p \to K^0\Lambda$, $\pi^- p \to K^0\Sigma^0$, and $\pi^+ p \to K^+\Sigma^+$ reactions is shown in Fig. 9 (Fig. 10). At present those data are available in the range $W \leq 2.4$ GeV. From the figures, one can observe that the kinematical coverage of the $\pi^- p \to K^0\Sigma^0$ is small. No differential cross sections are available from the threshold up to $W = 1.85$ GeV, and the $\cos\theta$ bins of P at each energy are very limited. Because of this, it is found [20] that the available $\pi^- p \to K^0\Sigma^0$ data are not enough to

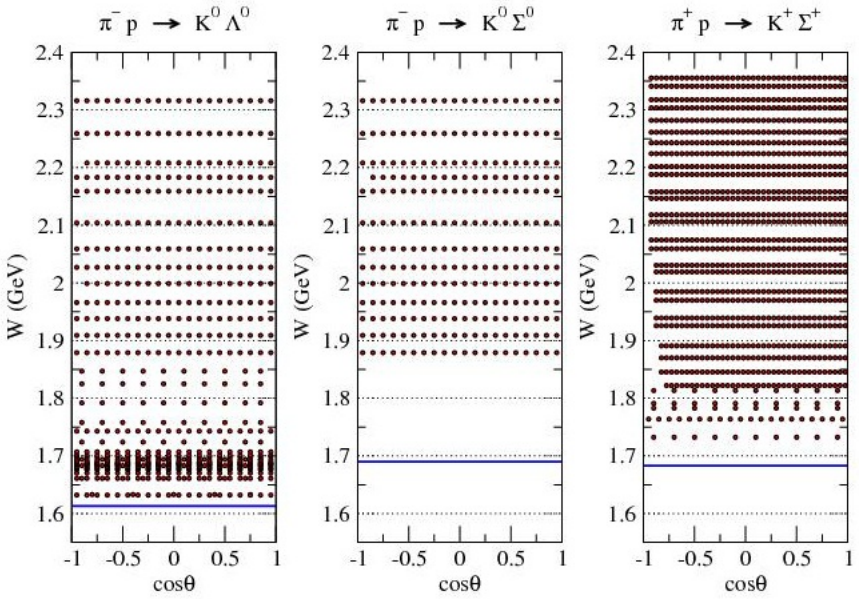

Figure 9: Kinematical coverage of the differential cross sections $d\sigma/d\Omega$ for $\pi^- p \to K^0\Lambda$, $\pi^- p \to K^0\Sigma^0$, and $\pi^+ p \to K^+\Sigma^+$. Blue lines represent the threshold energy of each reaction.

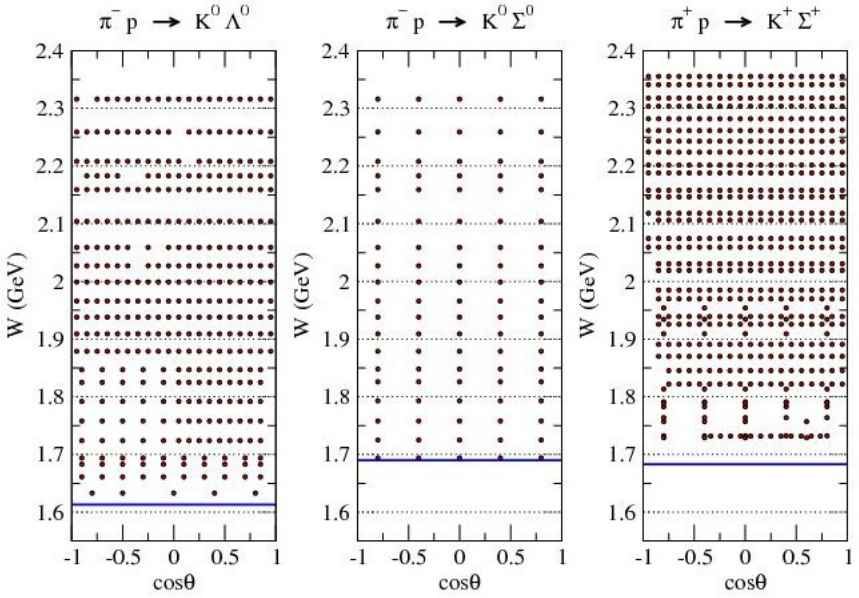

Figure 10: Kinematical coverage of the recoil polarization P for $\pi^- p \to K^0\Lambda$, $\pi^- p \to K^0\Sigma^0$, and $\pi^+ p \to K^+\Sigma^+$. Blue lines represent the threshold energy of each reaction.

Table 1: Masses and widths of the excited Δ^* baryons from various references.

Group	PWA	$\Delta(1600)$	$\Delta(1920)$
GWU [23]	πN	-	-
GWU [22]	πN	1457 - 400i	-
Bonn-Gatchina [24]	$\pi N, KY$	1480 - 120i	1930 - 150i
Julich [25]	$\pi N, KY$	1455 - 347i	2057 - 113i
EBAC [26]	πN	-	-
DCC [21]	$\pi N, KY$	1746 - 157i	-

provide critical constraints on the partial-wave analysis. Both $\pi^- p \to K^0\Sigma^0$ and $\pi^+ p \to K^+\Sigma^+$ data are necessary to determine $\pi N \to K\Sigma$ amplitudes of the isospin 1/2 and 3/2 states uniquely.

2.6 The special case of $\pi^+ p \to K^+\Sigma^+$

Between center-of-mass energies of 1.7 to 2.0 GeV, signals of some nucleon resonances are not clear from the pion-nucleon partial-wave amplitudes. Recent PWA studies of Arndt *et al.* put into doubt the resonances in this energy region [22].

The situation can be significantly improved by using the coupled-channel analysis approach, taking into account the open meson-baryon channels such as $\pi\pi N$ and KY. An important example is the $J^\pi = 3/2^+$ Δ resonances, where the $\Delta(1600)$ and $\Delta(1920)$ are listed as excited states of the $\Delta(1232)$. The former is considered as a 'Roper'-like (radial excitation) state of the $I = 3/2$ ground state, and its mass is of great importance to understand the 'Roper'-like excited baryons. The current situation of these resonances is summarized in Table 1.

The excited Δ^* is not seen (or only weakly seen) in the PWA studies based only on the πN amplitude, whereas these excited states are found when the KY channels are included. Here the $\pi^+ p \to K^+\Sigma^+$ channel plays important role. This reaction is purely $I = 3/2$ and the higher threshold energy of this reaction puts more emphasis on the higher mass resonances.

If the excitation energy of the reported $\Delta(1600)$ is indeed about 250 MeV (about a half of the 500 MeV excitation of the $N^*(1440)$ Roper resonance), then this is in contradiction to the expectation that the first nodal excitation of baryon resonances is about 500 MeV. However the pole positions of $\Delta(1600)$ scatter among the analyses.

The new data on $\pi N \to \pi\pi N$ and $\pi^+ p \to K^+\Sigma^+$ proposed here would be critical for resolving the ambiguity in the pole position of the Roper-like excitation, the $\Delta(1600)$. The $\pi\pi N$ data are needed to determine the

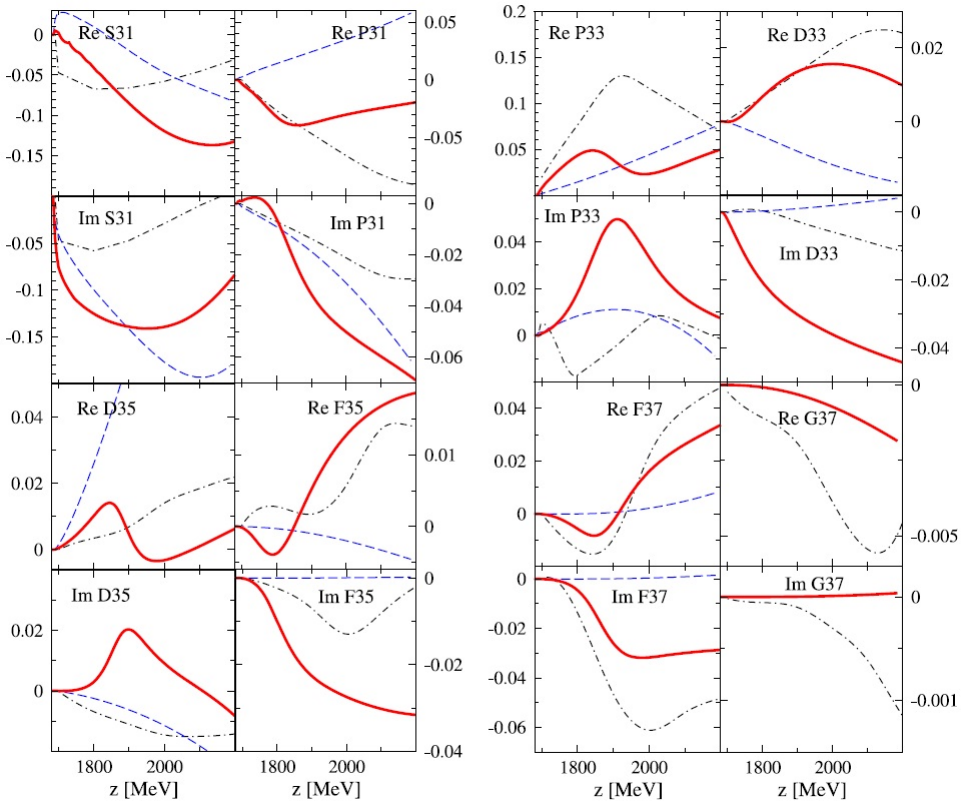

Figure 11: Partial wave amplitudes for the $\pi^+ p \to K^+\Sigma^+$ reaction from various models, from Ref. [25]. (See text for explanation of the curves.)

imaginary part of the pole position since only the πN and $\pi\pi N$ channels are open in the relevant energy region [21]. Similarly, it is important to include the $K^+\Sigma^+$ final state in the analysis of the Δ resonances to identify the spin $J = 5/2$ resonances. Precise data and theoretical progress is needed to clarify the excitation spectrum around the second resonance region.

To show the ambiguity that exists in the current data, Fig. 11 from the Julich theory group [25] shows the PWA solutions that exist from different models (all based on the same database). The solid line is a coupled-channels calculation, and the dashed lines show the same calculation with coupled-channels turned off. The dash-dotted curves are a PWA (without coupled-channels) from 1984. Clearly, there is quite a lot of disagreement between the curves, and the nucleon resonance parameters (mass and width) extracted from the different PWA solutions also differ. The importance of statistically precise data, which the proposed J-PARC measurements would provide, is very important to constrain the PWA solutions.

In the above paper, they conclude that "a wide $\Delta(1600)$ P_{33} has been

found" which is only tentatively identified by the PDG [6]. They continue "Furthermore, there is a clear need for the three-star $\Delta(1920)$ P_{33} resonance. This state is found to couple only weakly to πN but stronger to $K\Sigma$." The evidence for this higher-mass Δ resonance is only weakly found in PWA of πN elastic scattering. If we want to know the full spectrum of nucleon resonances, data for the strange decay channels is also needed.

3 Experiment

The proposed experiment will be carried out on the K1.8 beamline of the Hadron Hall of the J-PARC accelerator. **The primary goal** is to measure the $\pi N \to \pi\pi N$ reaction, and in particular to search for evidence of new baryon resonances through a dynamical coupled-channels PWA. **A secondary goal** is to gather data on the $\pi N \to KY$ reaction, which is needed because very little is known experimentally about N* resonances that couple to KY decay, and also because the $K^+\Sigma^+$ final state is key to analyses of Δ^* resonances, which decay into purely $I = 3/2$ channels.

The high-statistics photoproduction data from Jefferson Lab makes it even more compelling to get high-statistics hadronic data. Without hadronic data, a coupled-channels partial-wave analysis to search for new nucleon resonances is not sufficiently constrained. The simultaneous analysis of both hadronic and photoproduction data, however, is a powerful constraint on the PWA [26].

3.1 Beamline and Detector Setup

The layout of the proposed experiment is shown in Fig. 12. At the K1.8 beamline, pion beams of momenta between 0.6 and 2.0 GeV/c are possible with rates of about 10^6 pions per (6 second) spill. The momentum resolution, $\delta p/p$, is about 2×10^{-3} providing a narrow momentum bite, which is important for the partial-wave analysis. The beam enters into a large-acceptance TPC, which records all charged tracks produced from reactions in the liquid hydrogen target. Tracks in the forward direction (mostly high-momentum particles) continue through the Kurama spectrometer for high-resolution ($\delta p/p \sim 10^{-2}$) analysis. Particles with tracks only in the TPC are expected to have resolutions of about 10^{-2}, although this depends on details of the TPC final design.

A schematic view of the proposed TPC is shown in Fig. 13. The volume is filled with gas, such as Ar-CH_4, and particles produce ionized tracks. The ionized electrons drift downward due to an applied electric field of typically 150-200 V/cm. Due to diffusion in the transverse direction of the drifting electron, the track resolution is limited to about a few hundred microns. The

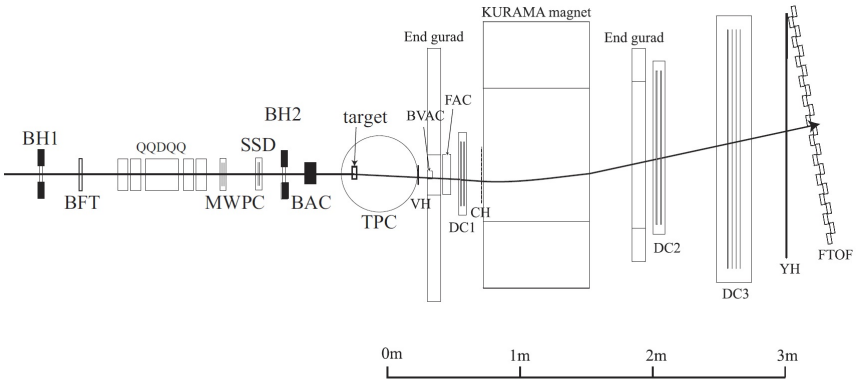

Figure 12: Schematic view of the experimental layout at the K1.8 beam line at J-PARC. The layout is the same as for the H-dibaryon search proposal (P42), with a large-acceptance TPC detector surrounding the target and the Kurama spectrometer for detection of high-momentum forward-going particles.

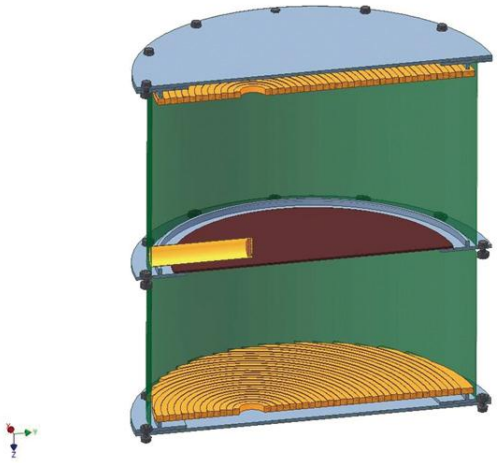

Figure 13: Cutaway view of the proposed TPC. The target is located off-center to provide better detection tracking for forward-going particles. Ionized tracks drift to the bottom. In the proposed experiment, the liquid hydrogen target will be inserted from the top.

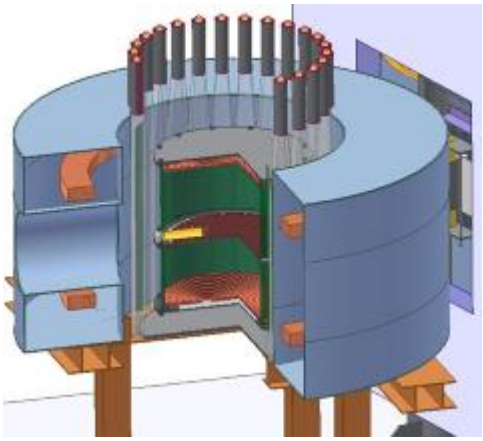

Figure 14: Schematic view of the TPC with Helmholtz coils and a scintillator hodoscope surrounding the active volume.

electrons are amplified using a multi-layer Gas Electron Multiplier (GEM) and read out using anode pads. Preliminary results from a TPC prototype (JAEA group) using 4 mm pads provided track residuals with good resolution. More development work on the TPC is needed, and simulations show that 1-2% resolution in momenta is obtained. The experiments proposed here can be done easily with that resolution.

The magnetic field for the TPC will be made using two superconducting Helmholtz coils, providing a field strength of about 1.0 Tesla and a field uniformity of better than 5%. A concept drawing is shown in Fig. 14. Also shown are plastic scintillator detectors around the TPC, which provide a fast trigger for the charged particles. In this experiment, we propose to have a prescaled two-track trigger and also a three-track trigger (not prescaled). More detail on the trigger and the event rates are given below. There will be a gap in the scintillator coverage for the incoming beam and also for the forward-angle tracks going into the Kurama spectrometer. A separate trigger will be set up for coincidences between the TPC and the spectrometer. In principle, the proposed measurements can be done with only the TPC, so if the spectrometer is moved from the K1.8 beamline, then still we can do the proposed measurements with the TPC.

The TPC electronics will be read out by a flash-ADC. The pad signals will be sent through a preamplifier and shaped to match the fADC sampling rate. The electronics design is not yet completed, and various designs are being studied by the JAEA group. It is essential for this experiment that data acquisition at high rates is possible, with event rates of 500-1000 per second. We do not expect this to be a limitation, since data acquisition technology has advanced rapidly in recent years.

Table 2: Previous published measurements of $\pi N \to \pi\pi N$ at lower W.

Reaction	**Maximum W**	**Reference**
$\pi^+ p \to \pi^+\pi^+ n$	1.35 GeV	Nucl. Phys. B 134, 413 (1978)
$\pi^+ p \to \pi^+\pi^+ n$	1.21 GeV	Phys. Rev. Lett. 66, 2569 (1991)
$\pi^+ p \to \pi^+\pi^0 p$	1.26 GeV	Phys. Rev. Lett. 72, 1156 (1994)
$\pi^\pm p \to \pi^\pm\pi^+ n$	1.24 GeV	Phys. Rev. C 58, 3419 (1998)
$\pi^\pm p \to \pi^\pm\pi^+ n$	1.24 GeV	Phys. Rev. Lett. 80, 1597 (1998)
$\pi^\pm p \to \pi^\pm\pi^+ n$	1.34 GeV	Zeit. Phys. C 48, 201 (1990)
$\pi^- p \to \pi^0\pi^0 n$	1.13 GeV	Phys. Rev. C 44, 956 (1991)
$\pi^- p \to \pi^+\pi^- n$	1.30 GeV	Phys. Rev. C 48, 981 (1993)

3.2 Yield Estimate

We make several assumptions for the event rates:

- Sample total cross section $\sigma_{\rm tot} = 2$ mb (=10^{-26} cm^2)
- pion beam rate $N_{\rm beam} = 10^6$ per (6 second) spill-cycle
- liquid hydrogen target length = 5 cm ($N_{\rm tgt} = 2.1 \times 10^{23}$ cm^{-2})
- TPC acceptance $A_{\rm det} = 0.5$ (about 0.7 for each particle).
- 100% computer livetime (using event buffering)

Using the formula for yield (or count rate)

$$Y = \sigma_{\rm tot} N_{\rm beam} N_{\rm tgt} A_{\rm det}$$

under the above assumptions, the event rate is approximately 200 events/spill-cycle. Factoring in the spill-cycle time, this becomes an *average rate* of about 2000 events per minute at this sample cross section.

We would like 40000 counts per angle bin, with 20 bins across $\cos(\theta_{cm})$, because we want to do multi-dimensional binning, and hence these 40000 counts get divided by the number of mass bins in each Dalitz plot. Assuming 400 bins in the Dalitz plot (20 bins by 20 bins in the two mass projections) then we would have 100 counts (a 10% uncertainty) per 2-dimensional mass bin at each center-of-mass angle.

According to the partial-wave analysis experts, it is recommended that we take small steps in W, of about 25-30 MeV, across the range of W from 1.5 to 2.15 GeV (corresponding to beam momenta from 0.73 GeV/c to 2.0 GeV/c). Below $W = 1.35$ GeV, there are some data that were taken as tests of chiral perturbation theory. A list of these lower-energy measurements are

		Cross Sections (mb) for pi- beam					
W (MeV)	p_{beam} (MeV/c)	$Tot_{Reaction}$(p pi-)	pi0 pi0 n	pi+ pi- n	pi0 pi- p	Hours	Shifts
1340	487.7	2.90	0.59	1.27	0.12		
1375	538.3	5.27	1.18	2.77	0.39		
1400	575.3	6.91	1.45	3.87	0.76		
1440	635.8	9.34	1.71	5.09	1.72		
1460	666.7	10.94	1.53	5.49	2.43		
1480	698.1	13.06	2.10	5.74	3.33		
1500	729.8	16.81	2.29	5.96	4.22		
1520	762.0	18.39	2.47	6.10	4.83	2.76	.60
1540	794.6	17.83	2.64	6.39	4.82	2.77	.60
1565	836.0	17.10	2.69	6.92	4.67	2.86	.61
1595	886.5	18.29	2.96	8.17	4.88	2.73	.59
1620	929.3	20.86	3.07	9.32	5.30	2.52	.56
1640	964.1	23.63	3.17	10.47	5.71	2.34	.54
1660	999.3	26.10	3.21	10.86	6.07	2.20	.52
1680	1034.8	26.69	2.79	10.68	6.28	2.12	.52
1700	1070.9	25.26	3.04	10.16	6.17	2.16	.52
1725	1116.5	22.91	2.53	9.12	5.89	2.26	.53
1755	1172.1	21.29	2.54	8.04	5.25	2.54	.57
1790	1238.2	20.90	1.68	7.21	4.50	2.96	.62
1830	1315.4	21.32	1.30	7.20	4.24	3.14	.64
1870	1394.3	21.90	1.80	7.74	4.54	2.94	.62
1910	1474.8	22.21	2.05	7.76	4.84	2.75	.59
1940	1536.4	22.00	2.00	7.75	4.50	2.96	.62
1970	1598.9	22.00	2.00	7.75	4.50	2.96	.62
2000	1662.4	22.00	2.00	7.75	4.50	2.96	.62
2025	1716.0	22.00	2.00	7.75	4.50	2.96	.62
2050	1770.3	22.00	2.00	7.75	4.50	2.96	.62
2075	1825.2	22.00	2.00	7.75	4.50	2.96	.62
2100	1880.8	22.00	2.00	7.75	4.50	2.96	.62
2125	1937.1	22.00	2.00	7.75	4.50	2.96	.62
2150	1994.1	22.00	2.00	7.75	4.50	2.96	.62
						Total	14.2

Figure 15: Table of cross sections (in mb) for the π^- beam, and hours to obtain 10^4 counts per angle bin at the given CM energy W for the lowest cross section to be measured.

		Cross Sections (mb) for pi+ beam				
W (MeV)	P_{beam} (MeV/c)	$Tot_{Reaction}$(p pi+)	pi0 pi+ p	pi+ pi+ n	Hours	Shifts
1340	487.7	0.74	0.01	0.00		
1375	538.3	1.03	0.52	0.10		
1400	575.3	1.40	0.70	0.16		
1440	635.8	2.33	1.20	0.25		
1460	666.7	2.98	1.48	0.29		
1480	698.1	3.78	1.99	0.35		
1500	729.8	4.73	2.57	0.44		
1520	762.0	5.87	3.32	0.56		
1540	794.6	7.26	4.54	0.72	18.52	2.6
1565	836.0	9.32	6.33	1.04	12.82	1.9
1595	886.5	11.64	8.57	1.51	8.83	1.4
1620	929.3	12.57	9.55	1.77	7.53	1.2
1640	964.1	12.74	9.81	1.77	7.53	1.2
1660	999.3	12.74	9.76	1.84	7.25	1.2
1680	1034.8	12.78	9.47	1.79	7.45	1.2
1700	1070.9	12.97	8.91	1.55	8.60	1.3
1725	1116.5	13.54	8.34	1.31	10.18	1.5
1755	1172.1	14.81	8.24	1.49	8.95	1.4
1790	1238.2	17.04	9.54	1.48	9.01	1.4
1830	1315.4	20.10	10.67	2.17	6.14	1.0
1870	1394.3	22.70	11.39	2.84	4.69	0.8
1910	1474.8	23.55	10.95	3.16	4.22	0.8
1940	1536.4	23.00	11.00	3.33	4.00	0.8
1970	1598.9	23.00	11.00	3.33	4.00	0.8
2000	1662.4	23.00	11.00	3.33	4.00	0.8
2025	1716.0	23.00	11.00	3.33	4.00	0.8
2050	1770.3	23.00	11.00	3.33	4.00	0.8
2075	1825.2	23.00	11.00	3.33	4.00	0.8
2100	1880.8	23.00	11.00	3.33	4.00	0.8
2125	1937.1	23.00	11.00	3.33	4.00	0.8
2150	1994.1	23.00	11.00	3.33	4.00	0.8
					Total	25

Figure 16: Same as previous figure, but for a π^+ beam.

Baker (1978)		Cross Section (mb)	(error)		J-PARC
W (GeV)	p_{beam} (MeV/c)	pi- p → K0 Λ		Hours	Counts
1.633	951.9	0.13	(0.02)	5.5	40,950
1.661	1001.0	0.46	(0.05)	4.9	128,340
1.683	1040.2	0.69	(0.07)	4.8	188,370
1.694	1060.0	0.92	(0.09)	4.8	251,160
1.724	1114.7	0.68	(0.10)	5.1	197,880
1.758	1177.7	0.48	(0.05)	5.7	156,960
1.792	1242.1	0.46	(0.05)	6.6	175,260
1.825	1305.7	0.25	(0.03)	7.1	102,750
1.847	1348.7	0.32	(0.03)	7.0	129,600
Saxon (1980)		**Cross Section (mb)**	**(error)**		
W (GeV)	**p_{beam} (MeV/c)**	**pi- p → K0 Λ**			
1.870	1395	0.25	(0.05)	6.6	95,250
1.900	1455	0.29	(0.06)	6.4	107,010
1.930	1515	0.22	(0.05)	6.2	78,540
1.959	1575	0.21	(0.04)	6.5	78,750
1.992	1645	0.16	(0.03)	6.6	60,960
2.020	1705	0.14	(0.03)	6.6	53,340
2.052	1775	0.13	(0.03)	6.6	49,530
2.097	1875	0.16	(0.03)	6.6	60,960
2.153	2000	0.15	(0.03)	6.6	57,150

Figure 17: Total cross sections (in units of mb) for $\pi^- p \to K^0\Lambda$ from the reference shown, and counts expected using the hours run to complete the measurement of $\pi p \to \pi\pi N$ in the previous tables.

Candlin (1983)		Cross Section (mb)	(error)		J-PARC
W (GeV)	p_{beam} (MeV/c)	pi+ p → K+ Σ+		Hours	Counts
1.813	1282	0.37	(0.02)	7	149,850
1.836	1328	0.41	(0.02)	6	141,450
1.861	1377	0.47	(0.03)	6	162,150
1.882	1419	0.52	(0.03)	5	148,200
1.917	1490	0.53	(0.03)	9	278,250
1.931	1518	0.55	(0.03)	9	288,750
1.962	1582	0.47	(0.03)	9	246,750
1.977	1614	0.49	(0.03)	9	257,250
2.012	1687	0.43	(0.02)	9	225,750
2.023	1712	0.44	(0.02)	9	231,000
2.052	1775	0.42	(0.02)	9	220,500
2.067	1808	0.39	(0.02)	9	204,750
2.099	1879	0.33	(0.02)	9	173,250
2.111	1906	0.37	(0.02)	9	194,250
2.140	1971	0.34	(0.02)	9	178,500
2.151	1997	0.30	(0.02)	9	157,500

Figure 18: Same as the previous figure but for $\pi^+ p \to K^+\Sigma^+$.

shown in Table 2. Also, the cross sections get smaller below 0.75 GeV/c and the beam time request starts to increase substantially. Experimentally, the electron contamination becomes an increasingly larger fraction of the beam at lower momenta. All of these factors have contributed to motivate 0.75 GeV/c as the lowest beam momentum for our proposal.

A table of total cross sections for the $\pi\pi N$ final states from the SAID database [27] are shown in Figs. 15 and 16 for the π^+ and π^- beams, respectively. The hours shown are calculated to obtain 40000 counts per angle bin at the given value of W for the lowest cross section to be measured here (which is $\pi^+p \to \pi^0\pi^-p$ and $\pi^+p \to \pi^+\pi^+n$, respectively). The final states will be measured simultaneously as long as they meet the trigger condition of two (or more) charged tracks in the TPC. Also shown is an estimate of the number of shifts needed to do these measurements (including time to change the beam momenta, see below), which totals about 14 shifts for the π^- beam and 25 shifts for the π^+ beam.

Although the beam tuning from one momentum setting to the next momentum is quick if the difference in beam momenta is small, occasionally it will require more time to retune the beamline. Also it will take time to set up the initial tune for each pion charge. Hence we request an extra 6 shifts for beam tuning, for a total of 45 shifts.

The reaction $\pi N \to KY$ reaction data can also be taken simultaneously with the above two-pion final state. The KY cross sections are smaller (typically by a factor of 10) and so the yield estimate for this reaction is smaller, as shown in Figs. 17 and 18. (Note: the beam momenta listed here are at the W values where previous data have been taken; these are not the same as the beam momenta in the previous tables for the $\pi\pi N$ final state and are listed here simply as examples of expected count rates.) Since this is a two-body final state, it is not necessary to do multi-dimensional binning. Hence the number of counts in each angle bin at a given W has thousands of counts (just divide the counts by 20, assuming 20 angle bins). Such data would allow for a PWA of the $\pi N \to KY$ reaction with higher precision than previously possible. (The uncertainty in the total cross section from the previous KY data is typically 10-30%, as shown in the fourth columns of Figs. 17 and 18.)

3.3 Trigger conditions

The trigger will be any two scintillators (there are 16 surrounding the TPC) that are both in coincidence with a beam particle hitting the target. Each of the $\pi\pi N$ final states have two charged particles except for the $\pi^-p \to \pi^0\pi^0n$ reaction. Since the beam momentum is known, the third particle can be identified by the technique of missing mass. (Care must be taken for background at lower beam momenta where electron contamination is larger.)

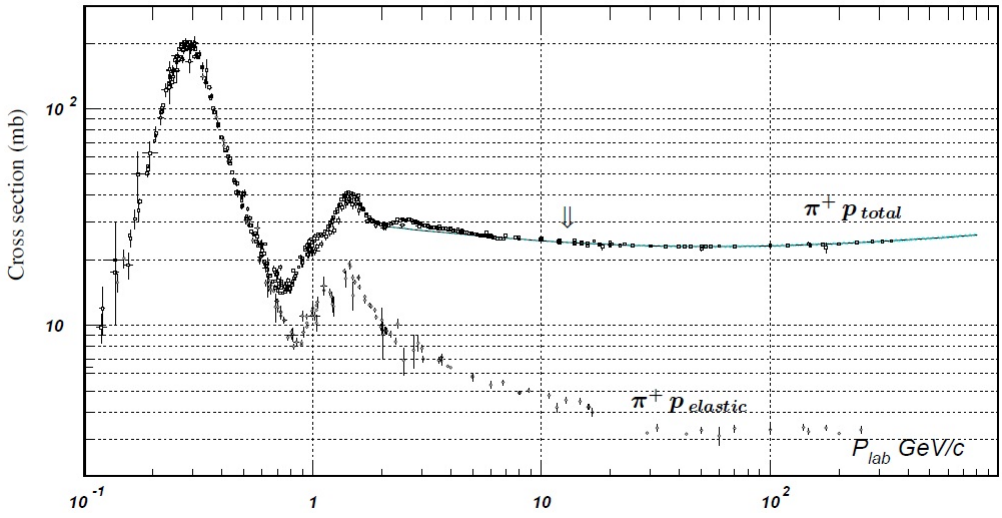

Figure 19: Total cross sections for a π^+ beam on a proton target, showing both total and elastic cross sections as a function of beam momentum [6].

The above trigger conditions are also satisfied by elastic $\pi N \to \pi N$ scattering, so the trigger rates will be higher than for the $\pi\pi N$ final state alone. Above about 0.9 GeV/c, the cross sections for elastic scattering are about half of the total cross section. At the beam momenta requested here, almost all of the inelastic cross section is to $\pi\pi N$ final states. Hence, above beam momenta of 0.9 GeV/c, we expect that about half of the triggers will be for elastic πN scattering, and the other half for $\pi N \to \pi\pi N$. Below 0.9 GeV/c, the trigger rate will be dominated by elastic scattering. Due to the dominance of the Δ resonance, the proposed measurements become increasingly difficult below about 0.65 GeV/c, as the trigger rate increases dramatically.

Based on the count rate assumptions in the previous section, and assuming a maximum cross section of 40 mb, the event rate will be 4000 events per spill cycle. The spill cycle is 6 seconds, but the beam hits the target for only 3 of the 6 seconds. Hence the instantaneous event rate will be about 4000/3 = 1333 events/second.

Event buffering can spread this rate over the full cycle, for a computer data acquisition rate of about 667/second, but in any case the TPC readout system must be able to work at the higher (instantaneous) rate. Using a flash-ADC running at 40 MHz and a commercial VME readout, these rates should be handled easily. A key step will be to implement zero-suppression in the readout, so as to read out only those pads that were "hit" by electrons from a charged track. Other TPC systems (such as the STAR detector) can handle very high count rates, and the proposed rates here are less.

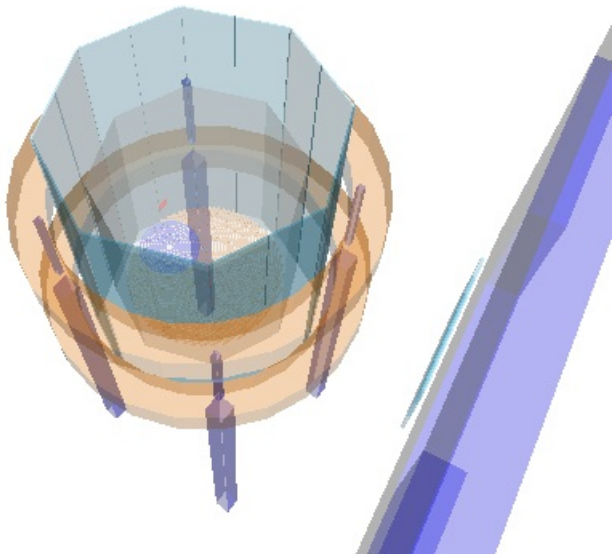

Figure 20: Computer-drawn schematic of the proposed TPC geometry used in geant4 simulations. See text for details of the geometry.

3.4 Detector simulations

Simulations for the $\pi N \rightarrow \pi\pi N$ reaction were done using geant4, using the same software as for the H-dibaryon search proposal (P42). A drawing of the geometry used is shown in Fig. 20, shown angled from a top view. The entrance to the spectrometer is shown in blue to the right of the figure. The radial pad design is shown at the bottom of the drawing. The target is a small orange spot centered above the radial pad axis. Four support posts holding up the Helmholtz coils are also visible due to the transparency of this drawing. The 16 trigger scintillators, in an octogon shape, are shown (in a dark cyan color) just inside the coils.

A new event generator was used for the above reaction, and the detector readout is done by smearing the track resolution according to the present TPC design. The simulations trigger required two charged tracks in the scintillator hodoscope, and the trigger efficiency was measured. Tracks that go straight up (into a cone with its axis directed along the TPC axis) are lost (unless an extra scintillator array is constructed above the TPC, which is not part of the original TPC design). Due to these losses, we find a detection efficiency of about 70% per particle. Precise values for the various $\pi N \rightarrow \pi\pi N$ reactions as a function of beam momentum are shown in Fig. 21 for the TPC geometry and trigger conditions described above.

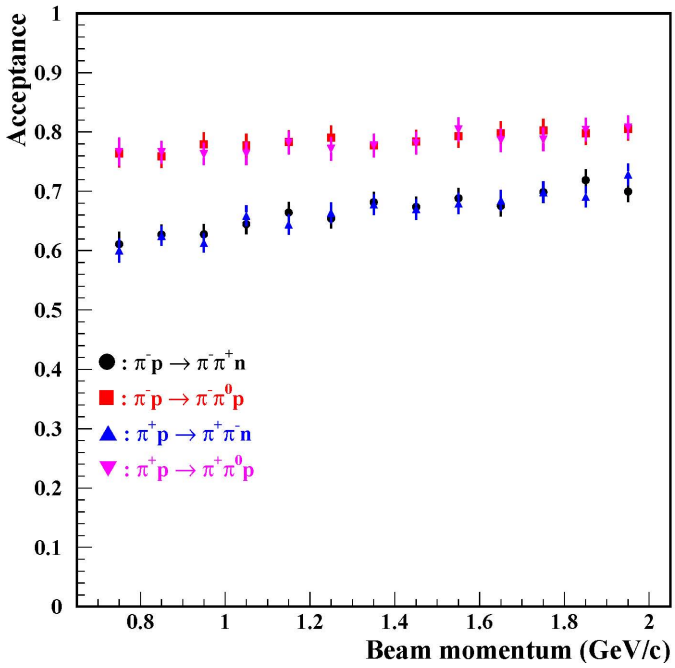

Figure 21: Detector acceptance for the reactions shown using the TPC geometry of the previous figure and the trigger conditions given in the text.

3.5 Systematic Uncertainties

One source of systematic uncertainty in the proposed experiment is the electron contamination in the beam. This contamination can be virtually removed by the beamline Cerenkov counter (1.7 atm isobutane gas). The cerenkov counter has a high efficiency, but it is not 100%, and the proper calibration of this detector is an important factor to determine the beam flux. This procedure is well known, and we expect a systematic uncertainty in the beam flux of only 1-2%.

Another source of systematic uncertainty is the target length and density. These factors can be controlled, and the latter calculated from the target temperature and pressure. Also, the windows of the target holder will account for some triggers, which can be subtracted by doing a few empty-target runs. We expect that the systematic uncertainty associated with the target will also be about 1-2%.

Particle mis-identification is another source of systematic uncertainty. This is difficult to predict until the TPC design is finalized. Preliminary simulations indicate that the energy loss as the particle passes through the TPC, along with the track curvature, can be used to cleanly separate pions from heavier particles. For the $\pi\pi N$ final state, we expect little uncertainty (at most a few percent) from particle mis-identification, provided that the geant4 simulations are properly tuned to reproduce experimental angular and momentum distributions. For the KY final state, kinematic constraints (due to the very narrow Λ and Σ widths) will reduce much of the uncertainty, but still this will need to be carefully modeled in the Monte Carlo. We again expect a few percent systematic uncertainty due to particle mis-identification of the KY reactions.

The trigger efficiency is perhaps the largest source of systematic uncertainty. The number of events where two charged tracks hit one scintillator (which will not satisfy the two-scintillator trigger condition) and the number of events where one of the charged tracks misses the scintillator ring are all sources of trigger inefficiency. Again, with proper tuning of the geant4 simulations to match experimental angle and momentum distributions, the trigger inefficiency can be calculated. At present, we do not have enough information to properly model the $\pi\pi N$ final state, and we must do the proposed measurements to get the experimental distributions. Nonetheless, we are confident that systematic uncertainties associated with the trigger efficiency can be kept less than 5% (and perhaps at the level of 1-2% after iteration of the event generator used in the simulations).

As mentioned above, πN elastic scattering will also satisfy the trigger conditions, and hence it will be part of the data stream. The πN elastic cross sections are know with good precision, and will serve as a useful calibration reaction for the experimental uncertainties. The high-statistics expected for

this calibration reaction will provide powerful constraints on the systematic uncertainties, especially for beam and target related quantities. The πN elastic events will also give valuable guidance to help tune the geant4 simulations to the TPC detector resolution. This gives us confidence that the systematic uncertainties can be kept low ($\sim 5\%$ or less).

4 Summary

With a modest beam-time request, an entire generation of data from the 1970s and 1980s for the $\pi N \to \pi\pi N$ and $\pi N \to KY$ reactions can be remeasured with much higher statistical and systematic precision. Because these data are necessary to the dynamical coupled-channels calculations that are now available to deduce the nucleon resonance spectrum, this is an opportunity that cannot be lost. J-PARC is the only facility in the world at present that can measure these important data.

The nucleon resonance spectrum provides a window into QCD. The new calculations being done on the lattice are now producing results that are a direct reflection of the underlying dynamics of QCD. As the calculations improve, it is important to confront the theoretical predictions with experimental data. However, precise data for photoproduction alone are not sufficient. Even though there has been a major effort by Jefferson Lab to take photoproduction data for this purpose, theoretical advances of coupled-channels calculations have shown that hadronic data are equally important to the goal of establishing the spectrum of nucleon resonances. The data on $\pi N \to \pi\pi N$ from decades ago, using older experimental techniques, are not sufficient for this purpose. In addition, data on $\pi N \to KY$ are also not very precise, but are important to find which nucleon resonances couple strongly to decays with strangeness. New data from J-PARC, requiring just 45 shifts of beamtime on the K1.8 beamline, could provide the precise cross sections that are needed.

Just as the spectrum of the hydrogen atom led to advances in the understanding of electromagnetism, the spectrum of nucleon resonances will provide a better understanding of non-perturbative QCD. One of the interesting predictions of the recent lattice calculations is the existence of hybrid baryons, where gluonic excitations add extra baryonic resonances not seen in the traditional quark model. Establishing new baryon resonances would be a major step forward in our understanding of QCD.

5 Appendix: the $\pi\eta N$ final state

In addition to the $\pi\pi N$ and KY final states, the proposed data will also contain data for the reaction $\pi N \to \pi\eta N$. As pointed out in a paper by

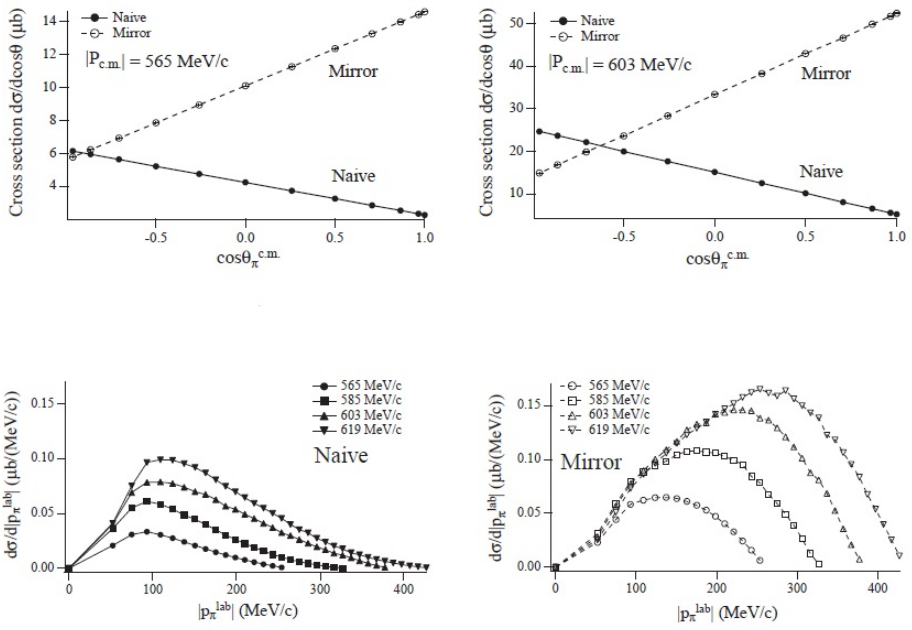

Figure 22: Angular (top) and momentum (bottom) distributions for two models of chiral symmetry as described in the text, from Ref. [28].

Jido, Oka and Hosaka [28], chiral symmetry of nucleon resonances can be studied by threshold $\pi\eta$ production.

Without going into the details of the theoretical models, for which details are given in Ref. [28], two models of chiral symmetry as applied to nucleons are called *naive* and *mirror* representations. These two models differ in their predictions of the coupling constant of the pion to the $N^*(1535)$ resonance, a well-known S_{11} resonance with $J = 1/2$ and opposite parity of the ground-state nucleon. The coupling constant $g_{\pi N^* N^*}$ where N^* is the $S_{11}(1535)$, has opposite sign in the naive model and in the mirror model. This can be observed physically from the angle and momentum distributions of the π^- in the final state. If the mirror representation is correct, then the $N^*(1535)$ is the chiral partner to the ground-state nucleon. This, in turn, has significant implications for the spectrum of nucleon resonances (*i.e.*, whether chiral partners are strongly coupled with opposite parity).

The experimental observables predicted by Jido, Oka and Hosaka [28] are shown in Fig. 22 for several beam momenta near threshold. The calculations are based on the effective Lagrangian model, using diagrams and equations given in that paper. The resulting angular distributions differ dramatically, with the mirror model favoring the forward pion angles and the naive model peaking at backward pion angles in the center-of-mass frame. This difference is also seen in the momentum distributions of the π^- in the lab frame, with

higher momenta favored in the mirror model.

One unknown parameter of the model is the magnitude of the coupling constant $g_{\pi N^* N^*}$. Ref. [28] assumes a fairly large value, on the same order as the pion-nucleon coupling $g_{\pi NN} \simeq 13$. Hence the magnitude of the cross sections shown in the figures, which are on the order of tens of microbarns near $p_\pi = 600 MeV/c$ (C.M. frame), but in reality it could be smaller. Since cross sections for the $\pi N \to \pi\eta N$ reaction have never been reported, it would be interesting to measure in any case. If the cross section is about 0.01 μb, then at a beam momentum of 0.60 GeV/c in the CM frame (=0.96 GeV/c in the lab frame), the average count rate would be 10 counts/minute. In a few hours of beam time, over 1000 counts would be measured (over the entire angular range) at each beam setting. Clearly, this measurement could be done if the cross section is as big as that predicted by Ref. [28].

While measurement of the $\pi N \to \pi\eta N$ reaction is not one of the primary goals of this proposal, it is worth mentioning that these data would come "for free" if the proposed $\pi\pi N$ data were taken with the TPC. It would be very interesting if we could measure the $\pi\eta N$ (using the missing mass technique) and hence answser some important questions about chiral symmetry in the nucleon resonance spectrum.

References

[1] S. Capstick and W. Roberts, Phys. Rev. D **49**, 4570 (1994).

[2] R. Koniuk and N. Isgur, Phys. Rev. D **21**, 1868 (1980).

[3] J.J. Dudek and R.G. Edwards, arXiv:1201.2349.

[4] A. Matsuyama, T. Sato and T.-S.H. Lee, Phys. Rep. **439**, 193 (2007).

[5] H. Kamano, B. Julia-Diaz, T.-S.H. Lee, A. Matsuyama and T. Sato, Phys. Rev. C **79**, 025206 (2009).

[6] K. Nakamura *et al.* (Particle Data Group), J. Phys. G **37**, 075021 (2010).

[7] N. Suzuki, B. Julia-Diaz, H. Kamano, T.-S.H. Lee, A. Matsuyama and T. Sato, Phys. Rev. Lett. **104**, 042302 (2010).

[8] M. Ripani *et al.* (CLAS Collaboration), Phys. Rev. Lett. **91**, 022002 (2003).

[9] D.J. Herndon *et al.*, Phys. Rev. D **11**, 3183 (1975).

[10] D. Mark Manley, Phys. Rev. D **30**, 536 (1984).

[11] J. Dolbeau, M. Neveu, F.A. Triantis and C. Coutures, Nucl. Phys. **B78**, 233 (1974).

[12] D.M. Manley, R.A. Arndt, Y. Goradia and V.L. Teplitz, Phys. Rev. D **30**, 940 (1984).

[13] L.D. Jacobs *et al.*, CERN Report CM-P00048050, CERN Libraries, 1971.

[14] R.D. Baker *et al.*, Nucl. Phys. **B141**, 29 (1978); D.H. Saxon *et al.*, Nucl. Phys. **B162**, 522 (1980).

[15] R. Bradford *et al.*, Phys. Rev. C **73**, 035202 (2006); M.E. McCracken *et al.*, Phys. Rev. C **81**, 025201 (2010).

[16] V.A. Nikonov, A.V. Anisovich, E. Klempt, A.V. Sarantsev and U. Thoma, Phys. Lett. *B662*, 245 (2008).

[17] L. Bachman *et al.*, Nucl. Phys. **B263**, 458 (1986).

[18] C. White *et al.*, Phys. Rev. D **49**, 58 (1994).

[19] T. Inoue *et al.* (HAL QCD Collaboration), arXiv:1112.5926[hep-lat].

[20] H. Kamano, S. Nakamura, T.-S. H. Lee, T. Sato, in preparation.

[21] H. Kamano, S. Nakamura, T.-S. H. Lee, Y. Oh, and T. Sato, in preparation.

[22] R. A. Arndt et al., Phys. Rev. C 74, 045205 (2006).

[23] R. A. Arndt et al., Phys. Rev. C 69, 035213 (2004).

[24] [3] A. V. Anisovich et al. Eur. Phys. J. A. 47 (2011), 27.

[25] [4] M. Doring et al., Nucl. Phys. A851 (2011) 58.

[26] [5] B. Julia-Diaz, T. -S. H. Lee, A. Matsuyama, and T. Sato, Phys. Rev. C76(2007) 065201.

[27] Center for Nuclear Studies, Data Analysis Services, George Washington University, http://gwdac.phys.gwu.edu.

[28] D. Jido, M. Oka and A. Hosaka, Prog. Theor. Phys **106**, 823 (2001).